Topics in Catalysis (2022) 65:383–391
https://doi.org/10.1007/s11244-021-01492-3

ORIGINAL PAPER

The Role of Counterions in Intermolecular Radical Coupling of Ru-bda Catalysts

Juan Angel de Gracia Triviño[1] · **Mårten S. G. Ahlquist**[1]

Accepted: 10 August 2021 / Published online: 19 August 2021

Abstract

Intermolecular radical coupling (also interaction of two metal centers I2M) is one of the main mechanisms for O–O bond formation in water oxidation catalysts. For Ru(bda)L_2 (H_2bda = 2,2′-bipyridine-6,6′-dicarboxylate, L = pyridine or similar nitrogen containing heterocyclic ligands) catalysts a significant driving force in water solution is the hydrophobic effects driven by the solvent. The same catalyst has been successfully employed to generate N_2 from ammonia, also via I2M, but here the solvent was acetonitrile where hydrophobic effects are absent. We used a classical force field for the key intermediate $[Ru^{VI}N(bda)(py)_2]^+$ to simulate the dimerization free energy by calculation of the potential mean force, in both water and acetonitrile to understand the differences and similarities. In both solvents the complex dimerizes with similar free energy profiles. In water the complexes are essentially free cations with limited ion paring, while in acetonitrile the ion-pairing is much more significant. This ion-pairing leads to significant screening of the charges, making dimerization possible despite lower solvent polarity that could lead to repulsion between the charged complexes. In water the lower ion pairing is compensated by the hydrophobic effect leading to favorable dimerization despite repulsion of the charges. A hypothetical doubly charged $[Ru^{VII}N(bda)py_2]^{2+}$ was also studied for deeper understanding of the charge effect. Despite the double charge the complexes only dimerized favorably in the lower dielectric solvent acetonitrile, while in water the separated state is more stable. In the doubly charged catalyst the effect of ion-pairing is even more pronounced in acetonitrile where it is fully paired similar to the 1+ complex, while in water the separation of the ions leads to greater repulsion between the two catalysts, which prevents dimerization.

Graphic Abstract

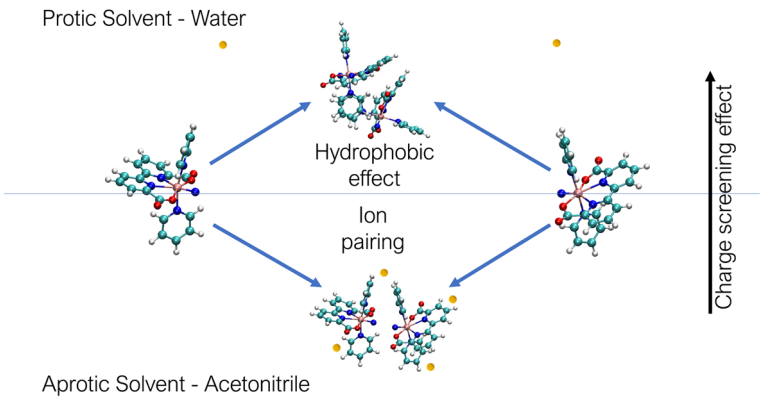

Keywords Solvent effects · Intermolecular radical coupling · Counterion effect · Catalysis · Aprotic solvents

✉ Mårten S. G. Ahlquist
ahlqui@kth.se

Extended author information available on the last page of the article

1 Introduction

Bimolecular association of ionic species is a well-known reaction in inorganic chemistry. Illustrative examples where counterions are involved are the inner- and outer-sphere electron transfer mechanisms. In the inner-sphere mechanism two complexes share a ligand to transfer the charge. In the outer-sphere mechanism the charge transfer happens by through-space electron-transfer. In both cases, the complexes can be positively or negatively charged, but they need to form contact complexes despite the possible Coulombic repulsion. The counterions can play a direct role in the inner-sphere mechanism as a ligand, e.g. in the reduction of $[Co(NH_3)_6]^{3+}$ with $[Cr(OH_2)_6]^{2+}$ where the second order rate constant is 8×10^{-5} dm^3 mol^{-1} s^{-1} in absence of chloride. Introducing Cl^- to the solvent leads to a ligand substitution at the Co complex which becomes $[CoCl(NH_3)_6]^{2+}$. The Cl^- attached to the Co can easily enter into the labile sphere of $[Cr(OH_2)_6]^{2+}$ generating a bridged transition complex with +4 charge and leading to a second order rate constant of 6×10^5 dm^3 mol^{-1} s^{-1}, thereby enhancing the reaction almost ten orders of magnitude[1]. In outer-sphere mechanism counterions can play a determinant role, nonetheless, do not directly participate in the reaction mechanism. The counterions instead reduce the dimerization free energy by decreasing the Coulombic repulsion. A well-documented example is the electron self-exchange between ferri- and ferrocyanide ions [2–4], $Fe(CN)_6^{3-}$ and $Fe(CN)_6^{4-}$. The electron transfer occurs via outer-sphere mechanism, meaning that anionic complexes need to be close enough to allow the electron transfer. Shorper [2] observed that the rate of the reaction increased adding cations in aqueous solution corresponding to the series H^+ to Cs^+ and Mg^{2+} to Sr^{2+}. The reasoning behind this behavior was explained by Kirby and Baker [5], the smaller ions get strongly attached to the water, leading to higher hydrated radii and increasing the solvent reorganization energy. Similar effects were also observed using acetic acid [3] which is also a protic polar solvent. Shorper [2] summarized the contributions of ion-pairing into three terms: the electrostatic term, the solvent reorganization term and the term related with the role of counterions in the electron transfer mechanism. The first two effects are the terms included in Marcus theory of the outer-sphere mechanism's free energy and the third one was investigated in the study. Shorper concluded that the electrostatic interaction had a noteworthy contribution and the counterions can affect in the electron transfer mechanism by facilitating ferro/ferricyanides pairing or serving as a conducting bridge for the electron transfer. Campion et al. [4] determined that the solvent reorganization effect is difficult to assess, and Kirby and Baker did not observe that counterions were serving as conducting bridges [6] leaving the pairing facilitation as the only possible contribution. More recently, solvent and counterion combined effects were addressed by Chaumont and Wipff [7]. They performed molecular dynamics simulations of Keggin anions in water and methanol (protic polar solvents) and found that in the pairing of the anions, hydrophobic and counterion effects have a significant impact. The hydrophobic effect is responsible of aggregation of apolar moieties in water. For Keggin anions in water π–π stacking were observed and characterized by a minimum in the potential mean force curve. In methanol no pairing was observed meaning that the hydrophobic effect in water is able to partially overcome the Coulombic repulsion. The counterion contribution was analyzed through its distribution in the Keggin ions dimer and a neutralization of the total negative charge was observed due to the distribution of the counterions on the surroundings of the dimer. The role of counterions in aprotic solvents, to the best of our knowledge, have not been studied before.

In the framework of this particular study, molecular catalysts offer a straightforward way to understand the relationship between structure and catalytic activity [8], and the role of solvent dynamic effects is central. Ru-bda is one of most studied molecular water oxidation catalysts (MWOCs), not only due to its excellent performance [9] also for some interesting features including a distorted 6-coordinate geometry which easily allows a 7-coordinate geometry, and the key role of carboxylate ligands in the stability and reactivity [8]. The development of this particular catalyst by Sun [10] was inspired by the oxygen evolving complex in photosystem II, where the carboxylate ligands can stabilize high-valent Mn states [11]. The key properties of this catalyst are, in addition to the mentioned distorted 6-coodination geometry, a second order kinetics with respect to the catalyst concentration, indicating an intermolecular interaction in the rate-limiting step [10, 12]. From the discovery of Ru-bda catalyst in 2009 several investigations in the mechanistic steps have been done, Privalov et al. proposed direct O–O coupling from two Ru^{IV}–O. radicals as O–O bond formation mechanism (the so called I2M mechanism) [12]. After that point many researchers have been explored the complete catalytic cycles and the key properties explaining reactivity and stability [8]. In our group we have explored the role of the solvent in the dynamics of Ru^{V}=O moieties and the nature of O–O bond formation barrier based on empirical valence bond theory (EVB) [13–17]. We found that the intrinsic barrier in the O–O bond formation between the two radicals is negligible and the formation of the prereactive dimer is determining the activity of the catalyst. In addition, solvation effects and the hydrophobic character of the oxo moiety are determinants in the formation of prereactive dimer [14] in aqueous solution. To exploit the hydrophobic effects on the I2M mechanism Sun

and co-workers introduced π-extended isoquinolines as axial ligands in the Ru-bda obtaining a significantly improved catalytic performance in water oxidation [18]. From molecular dynamics simulations we found that the π–π stacking interaction is driven by the water medium [14]. Additional studies performed by Sun's group indicated that increasing the hydrophobic effects, by adding halogen substituents (F and Br) on the axial ligands leads to better performance on the Ru-bda [19]. All these observations point in the direction of hydrophobic effects and π–π stacking interaction as a key driving force for the I2M mechanism.

Since we found that water has a key role in the dimerization of Ru-bda catalysts we were surprised by the study from Nakajima et al. [20], where production of N_2 from ammonia was assisted with Ru-bda catalyst using acetonitrile as solvent with second order kinetics. It was found that a key step was very similar to the O–O bond formation in water and involved coupling of two Ru–N intermediates. However, since experiments were carried out in acetonitrile, the formation of the prereactive dimer cannot be reliant on the hydrophobic effect. Moreover, the key intermediate is positively charged, and it is to be expected that the Coulomb repulsion should be more significant in a less polar solvent than water due to a lower charge screening. It is therefore not clear what drives the two catalysts to form the dimer in non-aqueous solvents and how the step differs from the corresponding reaction in water. We have performed classical MD simulations to understand the supramolecular effects in water and acetonitrile solvents. We also created artificially oxidized doubly charged complexes to further understand the effect of the overall charge on the formation of the prereactive dimer. Since radical coupling can overcome limitations of scaling relations of other mechanisms [21] understanding all aspects of this mechanism is key to development of highly reactive water and ammonia oxidation catalysts.

2 Results and Discussion

In order to determine the intermolecular effects behind the dimer formation we developed a force field model of $[Ru^{VI}N(bda)(py)_2]^{+1}$ founded on our recent OPLS-AA [22] based force field [14]. The bonded terms of ruthenium were adapted from our previous studies of $[Ru^{V}O(bda)(py)_2]^{+1}$ exception of those related to the nitrogen, and ESP charges were calculated for all atoms. The geometry of $[Ru^{VI}N(bda)(py)_2]^{+1}$ is similar enough to $[Ru^{V}O(bda)(py)_2]^{+1}$ to consider equivalent bonded parameters, and the nitride also has a close-to-zero charge similar to the oxo (Fig. 1) and is therefore also likely hydrophobic [15]. This common characteristic in localized hydrophobicity can partly explain the formation of the prereactive dimer in water but not in acetonitrile.

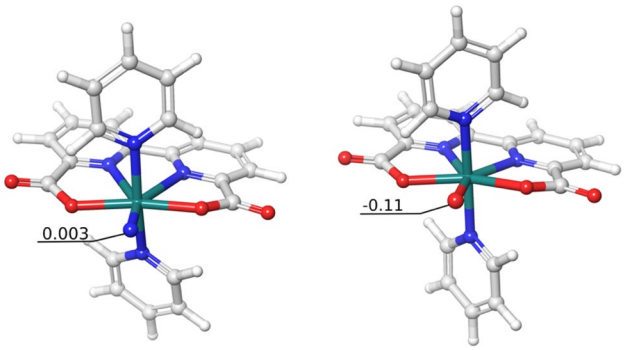

Fig. 1 Partial charge of nitride in $[Ru^{VI}N(bda)(py)_2]^{+1}$ (left) vs. partial charge of oxo group in $[Ru^{V}O(bda)(py)_2]^{+1}$ (right). Atom colours are respectively: Grey, white, red, blue, green—carbon, hydrogen, oxygen, nitrogen and ruthenium

For the study of the formation of the prereactive dimer we calculated the potential of mean force by performing umbrella sampling (US) simulations. The simulation periodic box had a size of 47.744 Å in each direction and the molecules were separated 18.55 Å (Ru–Ru distance) with each nitride pointing in a different direction to not bias the formation of the face-to-face geometry from the initial structure (Fig. 2). The simulation box was filled with SPC/E [23] water or with acetonitrile. US simulations were carried in an NPT ensemble to derive Gibbs free energies at 300 K.

We found from both profiles that the interaction is favorable (Fig. 3), but two details can be highlighted: Firstly, free energy needed to reach the interaction distance (around 11 Å) is similar in acetonitrile and in water and counterintuitively the encountering of catalysts is equally easy in a less polar solvent with an electrostatic repulsive interaction. Secondly, the prereactive minimum is at slightly different distances. In acetonitrile the minimum is closer than in water, and we therefore looked closer on the conformations to see if there is any difference between both solvents. Since the computed PMF is referred to the distance between the centroids of the catalysts we do not have information about the orientation and the catalysts could be paired in unproductive ways. We recently reported that the effect of hydrophobic/hydrophilic directionality affects the performance of Ru-catalyzed water oxidation due to the orientation of the catalysts during dimerization [17]. We calculated the radial distribution function (RDF) on the N–N intermolecular distances using the US simulation snapshots (thus, we have a statistically well weighted distribution) to get information on the most probable conformations. In Fig. 4 we observe different statistically predominant regions for each solvent and just by visualizing the simulation in those regions we observed two different conformations. In water, pyridine π–π stacking is the dominant conformation and, therefore, is more stable than the prereactive. So, the "driving force" in water

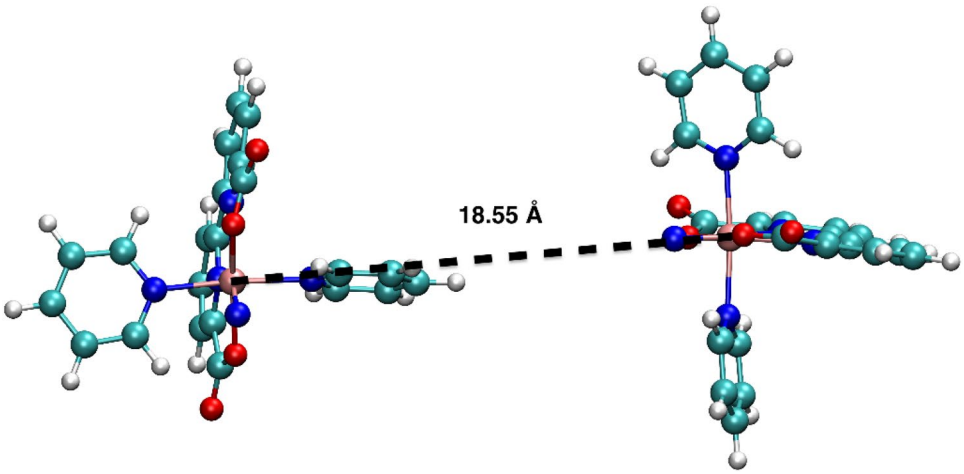

Fig. 2 Initial positions of the catalysts for US simulations

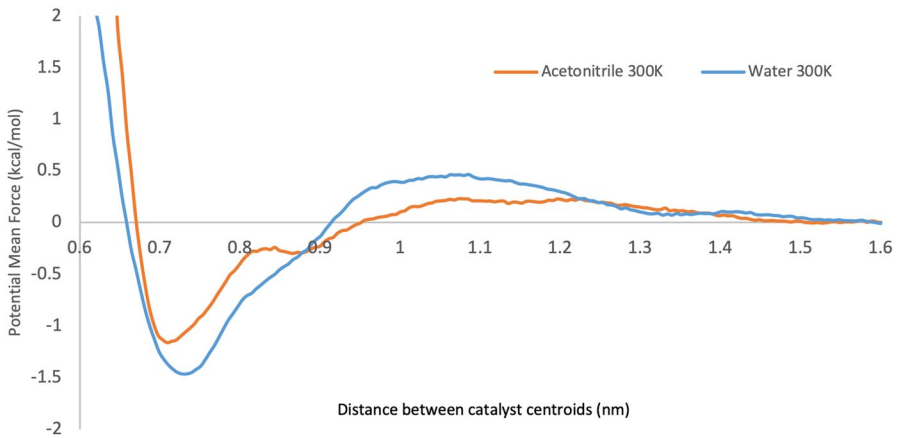

Fig. 3 Potential of mean force profile of the catalysts approaching in water and acetonitrile. The lines represent the free energy as the two catalysts are approaching using as reference for the distance the centroids of the molecules. The PMF have been corrected respect to the maximum distance, therefore, representing the relative free energy respect to the farthest distance

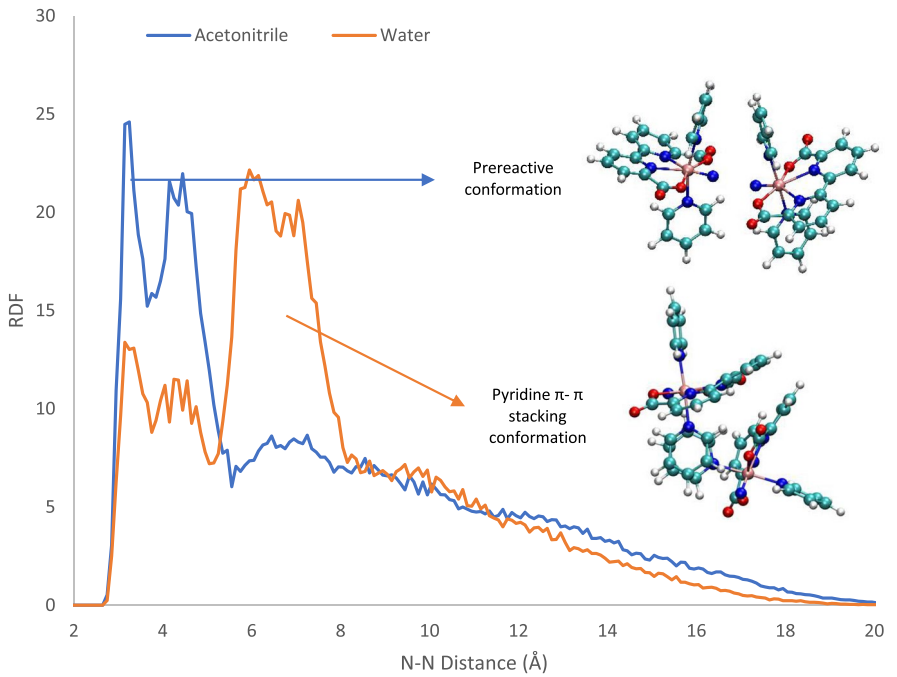

Fig. 4 Radial distribution function of nitride-nitride distance using the potential of mean force simulation snapshots in water and acetonitrile. The RDF have been computed using as reference one nitride and as a target the nitride of the other catalysts

is, as expected, the hydrophobic effect leading to stacking of the pyridines, but at the same time the axial π extended systems generate some resistance to reach the prereactive conformation. In acetonitrile the dominant conformation is the prereactive one, and the π–π stacking is not observed, indicating that a different effect is leading the dimerization process in acetonitrile.

In order to further investigate the interaction of the charged complexes in water and acetonitrile, we decided to amplify the Coulombic repulsion and create an artificial +2 charged complex. Acetonitrile has a relative polarity of 0.46 compared to water [24] and a dielectric constant [25] of 36.0 versus 80.2 for water [26] at 298.15 K, implying a low solvent-screening of charges. This consideration is important because electrostatic interactions are more significant in acetonitrile since lower dielectric constants leads to a lower screening of charges. We followed the same process as the single charge catalyst and the results on the PMF calculation are shown in Fig. 5. We find qualitatively different results for the doubly charged complex compared to the singly charged. In water the interaction is no longer favorable, and the dimer is not stable anymore. This indicates that the +2 charge on the catalysts the repulsion is significant enough in water to counterbalance the hydrophobic-effect/electrostatic-repulsion balance in favor of the latter. In acetonitrile the interaction becomes favorable even at longer distance. This observation indicates more markedly that something else should be playing a key role in the dimerization process. Counterions have been found to affect dimerization processes in protic solvents [1–7]. We therefore decided to study the behavior of the counterions in the protic and aprotic systems with the large hydrophobic ruthenium bda catalyst ions.

In our MD simulations, as a common practice, we added counterions to the solvent in order to create a neutral system and avoid non-convergence in particle mesh Ewald (PME) electrostatic field calculation [27]. Since catalysts are positively charged, Cl^- ions have been added to the solvent. In order to get quantitative data on solvent influence on catalyst-counterion interaction we studied the probability distribution of counterions around catalyst (considering Ru as the reference) in twelve systems: One catalyst +1 charged in water and in acetonitrile. One catalyst +2 charged in water and in acetonitrile. Two catalysts +1 charged in water and in acetonitrile dimerized and separated a minimum of 18 Å. Two catalysts +2 charged in water and in acetonitrile dimerized and separated a minimum of 18 Å.

2.1 Single Catalyst Counterion Distributions

For +1 charged catalyst in acetonitrile there is significant probability that the chloride ion is located within 10 Å from the Ru with 41 % of the cumulative probability (Fig. 6), which indicates a tendency to form a pair of charges and moving as a neutral set. This tendency can explain a lower free energy to set the catalysts close enough to form the prereactive dimer. Nevertheless, in water, the probability distribution is quite close to a Gaussian distribution (see Fig. S3) indicating a Quasi-Brownian motion, but vaguely overpopulated at shorter distances with only 7.4 % of the cumulative probability within 10 Å (Fig. 6).

In +2 charged systems (Fig. 7) tendencies are quite similar as +1, but since the charge is higher, the effect is more dramatic in acetonitrile with cumulative probability of 68.7 % below 10 Å and since there are two counterions per catalyst also the cumulative probability below 7 Å increases. That is because the counterion can be on the edge of the pyridine or/and the terpyridine. One question that arises is: how probable is to find two counterions in the same solvation shell? To that we calculated the probability of a new variable, the difference in between Ru-Cl^-_1 and Ru-Cl^-_2 distances (subindices are used just to distinguish the two

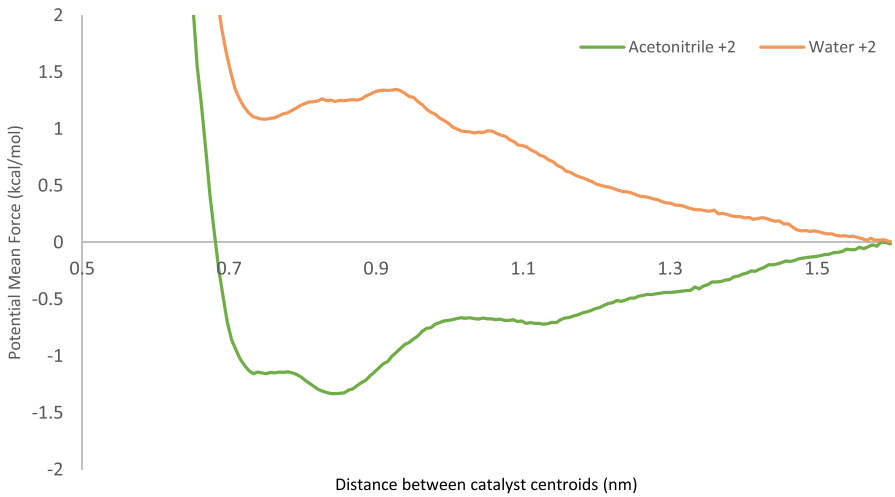

Fig. 5 Potential mean force profile of the +2 charged catalysts approaching in water and acetonitrile. The lines represent the free energy as the two catalysts are approaching using as reference for the distance the centroids of the molecules. The PMF have been corrected respect to the maximum distance, therefore, representing the relative free energy respect to the farthest distance

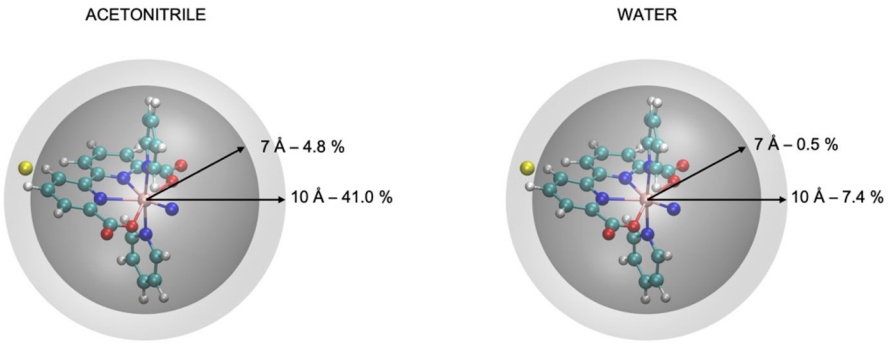

Fig. 6 Representation of the accumulated probability to find a counterion (yellow) at 7 Å and 10 Å when the catalyst is +1 charged in acetonitrile (left) and water (right)

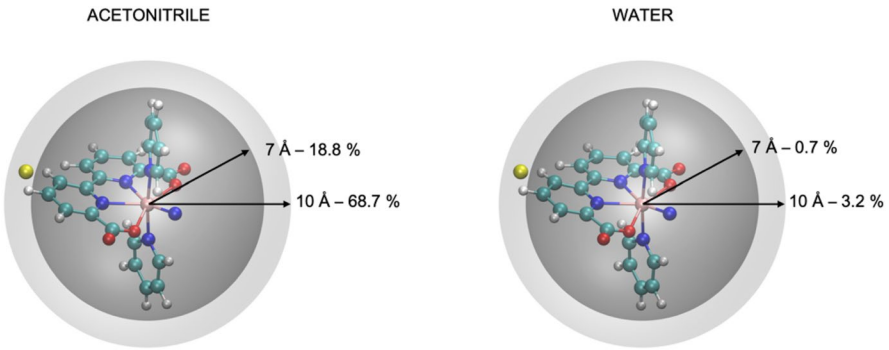

Fig. 7 Representation of the accumulated probability to find a counterion (yellow) at 7 Å and 10 Å when the catalyst is +2 charged in acetonitrile (left) and water (right)

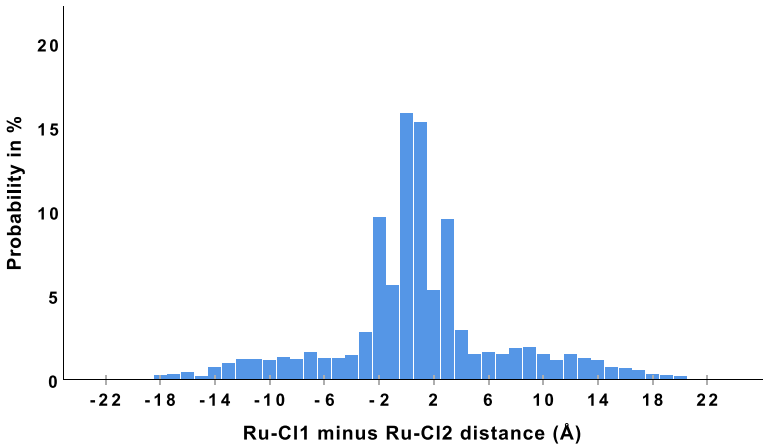

Fig. 8 Histograms of the probability distribution of the relative distance in between the two counterions respect to the ruthenium

ions). As we can see in the probability distribution (Fig. 8), the highest probability is in between 0 Å and 3 Å, this means that mainly both Cl^- are mainly located in the same solvation shell but also can be separated 3 Å (which is consistent with the two peaks observed at 5 Å and 8 Å in the probability distribution).

2.2 Two Catalysts Counterion Distributions

To further understand the dimerization process and the effect behind it we studied the counterion distribution around the two catalysts in one simulation box. In the simulations with two catalysts, we computed the distances and established a cutoff distance of 9 Å to consider the counterion paired with the catalyst. The choice of 9 Å as a cutoff distance comes from the peaks in the probability distributions for one catalyst (see S.I) Then, we counted the number of counterions with the following rule:

$$C_{ij} = \begin{cases} C_{ij} = 1 \;\; if \; d_{ij} \leq 9\text{Å} \\ C_{ij} = 0 \;\; if \; d_{ij} > 9\text{Å} \end{cases}$$

where C_{ij} is the counterion count for the ith counterion distance d_{ij} with the jth ruthenium. So, the total number of counts per snapshot is:

$$N = \sum_{j=1}^{2} \sum_{i=1}^{N_c} C_{ij}$$

where N_c is the total number of counterions, which are two for dimer of +1 complexes and four for dimer of +2 complexes. Finally, due to the possibility of numbers above N_c at short Ru–Ru distance (one counterion can be below the cutoff with respect to the two catalysts), we stablished the limit of $N \leq N_c$. The probabilities of N in the studied systems are shown in Table 1. Based on the result we can propose that the balance between a few effects is determining if the dimer formation is favorable or not (Figs. 4, 5 and 9). The hydrophobic effect is still the driving force in water, but the operational limit is +1 charged catalyst, since for +2 or higher the electrostatic repulsion leads to a significant decrease in the dimerization tendency. But in aprotic solvents like acetonitrile, we observed a reverse screening effect due to ion pairing, thus the repulsion is cancelled, and even longer-range attraction is observed. So, from the counterintuitive observation of a positive interaction in between charged catalysts in an aprotic solvent, we derived a novel effect of ion pairing that enables a completely new way to rational design of catalysts working via I2M mechanism, where highly charged states are accepted and even favored.

3 Conclusions

We have demonstrated the key role of counterions in the dimerization process of Ru-bda in acetonitrile, which is not only to diminish the expected electrostatic repulsion in between both charged catalysts but also leads to overall attractive interactions thanks to its capacity to pair and unpair. Moreover, the total charge of the catalyst favors the dimerization by enhancing the catalyst-counterion pairing. We believe that this understanding of the counterion effect in aprotic solvents opens for design of new catalysts for other applications that involves bimolecular steps. At the same time, we confirmed that the main effect driving the

Table 1 Probability of N in the systems studied dimer conformation vs separated catalysts

Counterions	Acetonitrile +1		Water +1	
	Separated (%)	Dimer (%)	Separated (%)	Dimer (%)
0	42.7	42.7	92.6	92.6
1	47.8	32.0	6.4	6.4
2	9.5	25.2	1.0	1.0
Counterions	Acetonitrile +2		Water +2	
	Separated (%)	Dimer (%)	Separated (%)	Dimer (%)
0	0.3	0.0	73.3	66.2
1	9.1	0.8	24.3	26.6
2	31.3	4.5	2.5	6.5
3	41.2	9.0	0.0	0.6
4	18.1	85.7	0.0	0.1

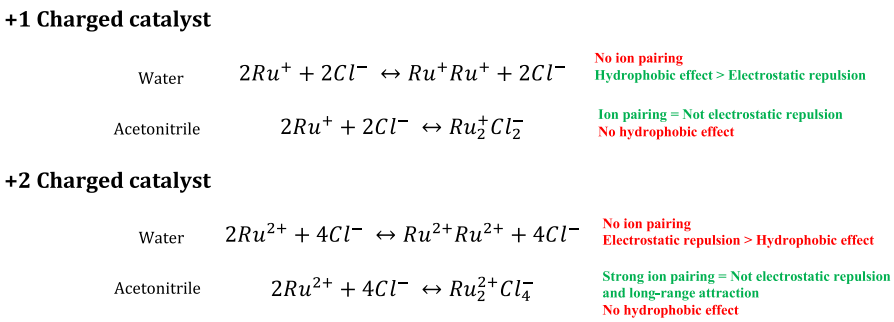

Fig. 9 Summary of the effects involved for the two solvents (water and acetonitrile) and schematic representation of the reactions. 2Ru refers to the free ruthenium complexes, Ru_2 is the dimerized complex in prereactive conformation, RuRu refers to the dimer in non-prereactive conformation. Cl refers to the chloride ions and Ru_2Cl_2 and Ru_2Cl_4 refers to the catalyst-counterion neutralized pairs. 2Cl or 4Cl indicates 2 or 4 free counterions

dimerization in water is the hydrophobic effect produced by the axial ligands. The counterions do not play a role in protic solvents due to the charge screening which leads to a Quasi-Brownian motion, meaning that counterions in water diffuses practically identical as water molecules (see S.I.). The hydrophobic effect can compensate the Coulombic repulsion when the charge is +1 in the catalysts, but for +2 the rate of the dimerization will be significantly lower hindering good performance of the catalyst. In protic water the low ion-pairing tendency will limit the possibility for using complexes with charges higher than 1+, which provides a guiding principle in the design of highly active water oxidation catalysts. In conclusion, we have showed how the dimerization of ionic catalysts lies in the balance between solvent effects (such as hydrophobic effect and charge screening), catalyst-catalyst Coulombic repulsion and catalyst-counterion coupling.

Supplementary Information The online version contains supplementary material available at https://doi.org/10.1007/s11244-021-01492-3.

Acknowledgements This research was financially supported by Vetenskapsrådet (VR 2018-05396) and the Knut & Alice Wallenberg (KAW) project CATSS (KAW 2016.0072). All calculations were performed on resources provided by the Swedish National Infrastructure for Computing (SNIC) at PDC Centre for High Performance Computing (PDC-HPC), High Performance Computing Center at Kungliga Tekniska Högskolan (KTH-PDC) in Stockholm through the project SNIC 2020/6-547, and the National Supercomputing Center under the project number SNIC 2021/5-42 and SNIC 2020/6-18 in Linköping, Sweden.

Author Contributions JADGT have conducted the calculations. MSGA have supervised the research. JADGT and MSGA wrote the manuscript.

Funding Open access funding provided by Royal Institute of Technology. Vetenskapsrådet (VR 2018-05396) and the Knut & Alice Wallenberg (KAW) project CATSS (KAW 2016.0072). All calculations were performed on resources provided by the Swedish National Infrastructure for Computing (SNIC) at PDC Centre for High Performance Computing (PDC-HPC), High Performance Computing Center at Kungliga Tekniska Högskolan (KTH-PDC) in Stockholm through the project SNIC 2020/6-547, and the National Supercomputing Center under the project number SNIC 2021/5-42 and SNIC 2020/6-18 in Linköping, Sweden.

Data Availability All the supporting data to elaborate this report and the computational details are available in the supporting information.

Declarations

Conflict of interest The authors declare no conflict of interest and non-financial interest.

References

1. Weller M, Weller MT, Overton T, Armstrong F, Rourke J (2018) Inorganic chemistry. Oxford University Press, Oxford
2. Shporer M, Ron G, Loewenstein A, Navon G (1965) Study of some cyano-metal complexes by nuclear magnetic resonance. II. Kinetics of electron transfer between ferri-and ferrocyanide ions. Inorg Chem 4(3):361–364. https://doi.org/10.1021/ic50025a022
3. Gritzner G, Danksagmüller K, Gutmann V (1976) Outer-sphere coordination effects on the redox behaviour of the Fe (CN) 63–/Fe (CN) 64 – couple in non-aqueous solvents. J Electroanal Chem 72(2):177–185. https://doi.org/10.1016/S0022-0728(76)80166-0
4. Campion RJ, Deck CF, King P, Wahl AC (1967) Kinetics of electron exchange between hexacyanoferrate (II) and (III) ions. Inorg Chem 6(4):672–681. https://doi.org/10.1021/ic50050a009
5. Kirby JF, Baker LCW (1998) Effects of counterions in heteropoly electrolyte chemistry. 1. Evaluations of relative interactions by NMR on Kozik salts. Inorg Chem 37(21):5537–5543. https://doi.org/10.1021/ic9713821
6. Kirby JF, Baker LCW (1995) Evaluations of a general NMR method, based on properties of heteropoly blues, for determining rates of electron transfer through various bridges. New mixed-mixed valence complexes. J Am Chem Soc 117(40):10010–10016. https://doi.org/10.1021/ja00145a011
7. Chaumont A, Wipff G (2012) Do Keggin anions repulse each other in solution? The effect of solvent, counterions and ion representation investigated by free energy (PMF) simulations. C R Chim 15(2–3):107–117. https://doi.org/10.1016/j.crci.2011.07.001
8. Zhang B, Sun L (2019) Ru-bda: unique molecular water-oxidation catalysts with distortion induced open site and negatively charged ligands. J Am Chem Soc 141(14):5565–5580. https://doi.org/10.1021/jacs.8b12862
9. Duan L, Wang L, Inge AK, Fischer A, Zou X, Sun L (2013) Insights into Ru-based molecular water oxidation catalysts: electronic and noncovalent-interaction effects on their catalytic activities. Inorg Chem 52(14):7844–7852. https://doi.org/10.1021/ic302687d
10. Duan L, Fischer A, Xu Y, Sun L (2009) Isolated seven-coordinate Ru (IV) dimer complex with [HOHOH]– bridging ligand as an intermediate for catalytic water oxidation. J Am Chem Soc 131(30):10397–10399. https://doi.org/10.1021/ja9034686
11. Lomoth R, Huang P, Zheng J, Sun L, Hammarström L, Åkermark B (2002) Styring S (2002) Synthesis and characterization of a dinuclear manganese (III, III) complex with three phenolate ligands. Eur J Inorg Chem 11:2965–2974. https://doi.org/10.1002/1099-0682(200211)2002:11%3c2965::AID-EJIC2965%3e3.0.CO;2-3
12. Nyhlén J, Duan L, Åkermark B, Sun L, Privalov T (2010) Evolution of O2 in a seven-coordinate RuIV dimer complex with a [HOHOH]– bridge: a computational study. Angew Chem Int Et 49(10):1773–1777. https://doi.org/10.1002/anie.200906439
13. Fan T, Zhan S, Ahlquist MSG (2016) Why is there a barrier in the coupling of two radicals in the water oxidation reaction? ACS Catal 6(12):8308–8312. https://doi.org/10.1021/acscatal.6b02697
14. Zhan S, Mårtensson D, Purg M, Kamerlin SCL, Ahlquist MSG (2017) Capturing the role of explicit solvent in the dimerization of RuV (bda) water oxidation catalysts. Angew Chem Int Et 56(24):6962–6965. https://doi.org/10.1002/anie.201701488

15. de Gracia Triviño JA, Ahlquist MSG (2020) Oxide relay: an efficient mechanism for catalytic water oxidation at hydrophobic electrode surfaces. J Phys Chem Lett 11(17):7383–7387. https://doi.org/10.1021/acs.jpclett.0c02009
16. Yi J, Zhan S, Chen L, Tian Q, Wang N, Li J, Xu W, Zhang B, Ahlquist MSG (2021) Electrostatic interactions accelerating water oxidation catalysis via intercatnteractions accelerating water oxidation catalysis via intercatalyst O–O coupling. J Am Chem Soc 143(6):2484–2490. https://doi.org/10.1021/jacs.0c07103
17. Zhan S, Zhang B, Sun L, Ahlquist MSG (2020) Hydrophobic/hydrophilic directionality affects the mechanism of Ru-catalyzed water oxidation reaction. ACS Catal 10(22):13364–13370. https://doi.org/10.1021/acscatal.0c02852
18. Duan L, Bozoglian F, Mandal S, Stewart B, Privalov T, Llobet A, Sun L (2012) A molecular ruthenium catalyst with water-oxidation activity comparable to that of photosystem II. Nat Chem 4(5):418–423. https://doi.org/10.1038/nchem.1301
19. Wang L, Duan L, Wang Y, Ahlquist MSG, Sun L (2014) Highly efficient and robust molecular water oxidation catalysts based on ruthenium complexes. Chem Commun 50(85):12947–12950. https://doi.org/10.1039/c4cc05069j
20. Nakajima K, Toda H, Sakata K, Nishibayashi Y (2019) Ruthenium-catalysed oxidative conversion of ammonia into dinitrogen. Nat Chem 11(8):702–709. https://doi.org/10.1038/s41557-019-0293-y
21. Craig MJ, Coulter G, Dolan E, Soriano-López J, Mates-Torres E, Schmitt W, García-Melchor M (2019) Universal scaling relations for the rational design of molecular water oxidation catalysts with near-zero overpotential. Nat Commun 10(1):1–9. https://doi.org/10.1038/s41467-019-12994-w
22. Jorgensen WL, Maxwell DS, Tirado-Rives J (1996) Development and testing of the OPLS all-atom force field on conformational energetics and properties of organic liquids. J Am Chem Soc 118(45):11225–11236. https://doi.org/10.1021/ja9621760
23. Berendsen HJC, Grigera JR, Straatsma TP (1987) The missing term in effective pair potentials. J Phys Chem 91(24):6269–6271. https://doi.org/10.1021/j100308a038
24. Reichardt C, Welton T (2011) Solvents and solvent effects in organic chemistry. Wiley, Hoboken
25. Khimenko MT, Aleksandrov VV, Gritsenko NN (1973) Polarizability and radii of molecules of some pure liquids. Zh Fiz Khim 47:2914
26. Archer DG, Wang P (1990) The dielectric constant of water and Debye-Hückel limiting law slopes. J Phys Chem Ref Data 19(2):371–411. https://doi.org/10.1063/1.555853
27. Ibragimova GT, Wade RC (1998) Importance of explicit salt ions for protein stability in molecular dynamics simulation. Biophys J 74(6):2906–2911. https://doi.org/10.1016/S0006-3495(98)77997-4

Authors and Affiliations

Juan Angel de Gracia Triviño[1] · Mårten S. G. Ahlquist[1]

[1] Departament of Theoretical Chemistry and Biology, School of Engineering Sciences in Chemistry Biotechnology and Health, KTH Royal Institute of Technology, 10691 Stockholm, Sweden